Cardiovascular Research (2011) **92**, 348–357
doi:10.1093/cvr/cvr217

Decreased nNOS in the PVN leads to increased sympathoexcitation in chronic heart failure: role for CAPON and Ang II

Neeru M. Sharma[1], Hong Zheng[1], Parmender P. Mehta[2], Yi-Fan Li[3], and Kaushik P. Patel[1]*

[1]Department of Cellular and Integrative Physiology, University of Nebraska Medical Center, Omaha, NE 68198-5850, USA; [2]Department of Biochemistry and Molecular Biology, University of Nebraska Medical Center, Omaha, NE 68198-5850, USA; and [3]Division of Basic Biomedical Science, College of Medicine, University of South Dakota, Vermillion, SD 57069, USA

Received 15 March 2011; revised 1 July 2011; accepted 5 August 2011; online publish-ahead-of-print 10 August 2011

Time for primary review: 47 days

Aims Previously, we showed an enhanced excitatory (*N*-methyl D-aspartate receptor-NR_1) and decreased inhibitory neuronal nitric oxide (NO) synthase (nNOS) influence within the paraventricular nucleus (PVN) of rats with chronic heart failure (CHF). Although NR_1 and nNOS are normally linked, they can be disconnected by nNOS sequestering with nNOS-associated protein (CAPON). The aim of this study was to elucidate the underlying mechanism for the disconnection between increased expression of NR_1 and decreased nNOS in the PVN of rats with CHF which leads to enhanced sympathoexcitation.

Methods and results CAPON expression was augmented while nNOS expression was decreased in the PVN of rats with CHF (6–8 weeks after left coronary artery ligation). Angiotensin II (Ang II) type I receptor (AT_1) antagonist losartan (Los) treatment in rats with CHF reduced renal sympathetic nerve activity with concomitant normalization of protein expression of CAPON and nNOS in the PVN. Los treatment also reversed the blunting of endogenous NO-mediated sympatho-inhibition in rats with CHF. Moreover, Ang II-induced increase in CAPON expression in NG108 neuronal cells was also ameliorated by Los.

Conclusion Blocking AT_1 receptors prevents the overexpression of CAPON and concomitant decrease in nNOS in the PVN, resulting in attenuation of sympathoexcitation commonly observed in CHF. Taken together, our data highlight the importance of altered expression and subsequent interaction of nNOS and CAPON within the PVN, leading to increased sympathoexcitation in CHF. Identifying this crucial nNOS/CAPON interaction regulated by AT_1 receptors may provide an important potential therapeutic target in CHF.

Keywords Sympathetic nerve activity • nNOS • CAPON • Chronic heart failure • Paraventricular nucleus

1. Introduction

Chronic heart failure (CHF) condition is characterized by an increased neurohumoral drive. Despite major advances in therapy, the exaggerated neurohumoral drive causes significant cardiovascular complications that contribute to increased morbidity and mortality. The increased sympathoexcitation has been shown to occur in both humans[1] and animal models[2,3] of CHF. With regard to the humoral activation during CHF, plasma levels of angiotensin II (Ang II), vasopressin, and endothelin have been shown to be increased in both humans[4] and animals.[5] The increased sympathoexcitation that occurs during CHF is thought to originate in the central nervous system (CNS).[6] In particular, the paraventricular nucleus (PVN) of the hypothalamus has been identified as a key integrating site involved in sympathoexcitation in CHF.[7]

Neuroanatomical, electrophysiological, and functional studies have indicated an important role for the PVN in cardiovascular regulation.[8,9] A number of different neurotransmitter systems have been shown to converge at the PVN to influence its neuronal activity.[8] This increased sympathoexcitation in CHF is due, in part, to increased

* Corresponding author: Department of Cellular and Integrative Physiology, University of Nebraska Medical Center, 985850 Nebraska Medical Center, Omaha, NE 68198-5850, USA. Tel: +1 402 559 8369; fax: +1 402 559 4438, Email: kpatel@unmc.edu

glutamatergic mechanisms in the PVN.[2] In particular, *N*-methyl D-aspartatic acid (NMDA) microinjection into the PVN produces exaggerated increases in renal sympathetic nerve activity (RSNA) in CHF consistent with an enhanced expression of the NR_1 subunit of the NMDA receptor in the PVN of CHF rats.[2] In terms of the inhibitory side of the equation, nitric oxide (NO) in the PVN has been shown to play an important inhibitory role in the regulation of sympathetic outflow.[10] Blocking the production of endogenous NO in the PVN results in an increase in RSNA, and this response is blunted in rats with CHF, suggesting that the endogenous NO mechanism is defective in CHF. Moreover, this NO-mediated inhibition in the PVN appears to utilize a γ-aminobutyric acid (GABA)-mediated mechanism that is also blunted in rats with CHF.[11] Taken together, these previous studies suggest that an imbalance between the overactivated excitatory glutamatergic system and blunted inhibitory NO/GABA mechanisms within the PVN may contribute to the sympathoexcitation commonly observed in CHF.[11]

There is actually a strong link between NMDA receptor activation and NO release.[12] NMDA receptor and neuronal NO synthase (nNOS) are linked through an intermediary adaptor protein PSD95 (post-synaptic density 95) for NMDA receptor-mediated calcium influx and nNOS activation.[13] This interaction between PSD95 and nNOS is mediated via a unique PDZ (post-synaptic density-95/drosophila discs large/zona occludens-1) domain.[14,15] CAPON (carboxy-terminal PDZ ligand of nNOS), first identified in rat brain neurons,[13] is a highly conserved protein with 92% sequence homology between rat and humans. CAPON consists of an N-terminal phosphotyrosine-binding (PTB) domain and a C-terminal PDZ-binding domain.[13,16] In the brain, CAPON competes with PSD95 for interaction with nNOS, and overexpression of CAPON prevents NMDA–nNOS interaction, suggesting that it acts as a negative regulator of NO production and its downstream signalling events.[13]

Elevated levels of Ang II in CHF[17] are of particular interest since Ang II has peripheral actions at the nerve terminals as well as central actions in the CNS to increase sympathoexcitation.[18] Further, angiotensin-converting enzyme inhibitor[19] as well as Ang II receptor blockers[18] are effective in reducing sympathoexcitation during CHF. In addition, Ang II microinjected into the PVN causes exaggerated increases in RSNA, mean arterial pressure (MAP), and heart rate (HR) in rats with CHF which appears to be due to increased expression of Ang II type 1 (AT_1) receptors,[18] although it may also be due to increased circulating levels of Ang II in CHF. Moreover, Ang II also has more long-term or chronic actions in CNS regions that are manifested through changes in gene and protein expression and enzyme activities.[20]

Previously, we showed a decrease in nNOS[11] and an increase in expression of the NMDA receptor subunit NR_1^2 in the PVN of rats with CHF. Moreover, losartan (Los), an AT_1 receptor blocker, treatment in rats with CHF restored sympathetic nerve activity and normalized (prevented) the changes in expression of NMDA-NR_1,[21] suggesting that AT_1 receptor activation may be linked to the reciprocal changes in NMDA-NR_1 and nNOS in the PVN. To further elucidate the underlying mechanism of down-regulation of nNOS, with a concomitant up-regulation of NMDA-NR_1 receptors, we examined the expression of nNOS and CAPON in the PVN of rats with CHF before and after Los treatment. Moreover, we examined the functional responses of changes in RSNA to NOS blockade within the PVN. Furthermore, we examined the effect of Ang II on expression of nNOS and CAPON in NG108 neuronal cell line as an *in vitro* model. Here, we report that Ang II affects the levels of both CAPON (increase) and nNOS (decrease) in the PVN of rats with CHF as well as in NG108 cells, *in vitro*. The changes in CAPON and nNOS are inversely related, possibly creating an imbalance in the excitatory/inhibitory interaction within the PVN, resulting in the sympathoexcitation that is commonly observed in the late stages of CHF.

2. Methods

2.1 Animals

Male Sprague–Dawley rats weighing 250–280 g (Sasco Breeding Laboratories, Omaha, NE, USA) were fed and housed according to approved guidelines of the University of Nebraska Medical Center Institutional Animal Care and Use Committee, which conforms to the Guidelines for the Care and Use of Laboratory Animals of the National Institutes of Health and the American Physiological Society.

2.2 Induction of heart failure

CHF was induced by ligation of the left coronary artery, as described previously.[6,17,18,21,22] Briefly, rats were ventilated at a rate of 60 breaths/min with 2–3% isoflurane during the surgical procedure. A left thoracotomy was performed through the fifth intercostal space, the pericardium was opened, the heart was exteriorized, and the left anterior descending coronary artery was ligated. Rats were randomly assigned to either the sham-operated control group or the CHF group. Left ventricular dysfunction was assessed using haemodynamic and anatomic criteria. Following 3 weeks of Los administration, echocardiograms were performed to measure left ventricular end-systolic diameter (LVESD), left ventricular end-diastolic diameter (LVEDD), and ejection fraction (EF). Left ventricular end-diastolic pressures (LVEDP) were measured using a Mikro-Tip catheter (Millar Instruments, Houston, TX, USA) inserted into the left ventricle via the right carotid artery. To measure infarct size, the heart was dissected free of adjacent tissues, and atria were removed. The right ventricle was opened with a lengthwise incision such that the heart was flattened with the left ventricle lying in the middle with the right ventricle on either side of it. The right ventricle was removed and the remaining left ventricle laid flat. A digital image of the left ventricle was captured using a Kodak DC290 digital camera (Kodak, Rochester, NY, USA) and the infarcted area and total left ventricular area quantified using SigmaScan Pro. Infarct size (%) was determined by dividing the size of the infarcted area by the total size of the left ventricle. Rats with elevated LVEDP ($\geq$15 mmHg) and infarct size $>$30% of the total left ventricular wall were considered to be in CHF.

2.3 Los treatment

Three weeks following coronary artery ligation, two subgroups of rats (Los-treated sham and Los-treated CHF) were treated with 10 mg/kg/day Los (Merck, Whitehouse Station, NJ, USA)[23] in the drinking water for a period of 3 weeks. Water intake was monitored, and subsequently, the Los was added to correctly dose the animals.

2.4 General surgery for haemodynamic and RSNA measurement and microinjection

Experiments were performed 6 to 8 weeks after CHF surgery. Rats were anaesthetized with urethane (0.75 g/kg ip) and α-chloralose (70 mg/kg ip). The left femoral vein was cannulated with polyethylene tubing (PE-50) for injection of supplemental anaesthesia. To maintain an adequate plane of anaesthesia, haemodynamic signals, such as MAP and HR, were used as an index for quantitative evaluation of the level of anaesthesia as well as for the absence of response to paw pinch. The left kidney was exposed through a retroperitoneal flank incision, and a branch of the renal nerve was isolated from the adipose and connective tissues. The distal end of

the nerve was placed on a bipolar platinum electrode after the ligation. The nerve–electrode junction was insulated electrically from the surrounding tissues with gel (Wacker, St Louis, MO, USA). The electrical signal was amplified with a Grass amplifier with high- and low-frequency cut-offs of 1000 and 100 Hz, respectively. The rectified output from the amplifier was displayed using the PowerLab system to record and integrate the raw nerve discharge. Basal nerve activity was determined at the beginning of the experiment. The RSNA recorded at the end of the experiment (after the rat was injected with hexamethonium, 30 mg/kg iv) was defined as background noise. The value of RSNA was calculated by subtracting the background noise from the actual recorded value, and changes found in integration of the nerve discharge during the experiment were expressed as a percentage from the basal value. The maximum RSNA was determined by injecting 20 μg of sodium nitroprusside iv in the femoral vein. The left femoral artery was cannulated to record the MAP and HR.[18]

For the placement of microinjection cannulas into the PVN, the anaesthetized rat (urethane 0.75 g/kg, α-chloralose 70 mg/kg ip) was placed in a stereotaxic apparatus (David Kopf Instruments, Tujanga, CA, USA). A longitudinal incision was made on the head, and the bregma was exposed. A small burr hole was made in the skull to allow access to the PVN. The coordinates for the PVN, determined with the Paxinos and Watson[24] atlas, were 1.5 mm posterior to the bregma, 0.4 mm lateral to the midline, and 7.8 mm ventral to the dura. A thin needle (0.2 mm OD) connected to a 0.5 μL microsyringe (Hamilton, Reno, NV, USA) was lowered into the PVN. N^G-monomethyl-L-arginine (L-NMMA) was injected into the PVN in three doses (50, 100, and 200 pmol) in a random order. Each animal received all three doses of L-NMMA. Subsequent injections were made at least 20 min after prior injections to allow MAP, HR, and RSNA to return to basal levels.

2.5 Micropunch of the PVN

A separate group of animals was euthanized by overdose of pentabarbital (65 mg/kg ip) and the brains were removed and quickly frozen on dry ice. Six serial coronal sections (100 μm) of the brain were cut using a cryostat. The PVN was bilaterally punched using the Palkovits technique[25] as described previously.[18]

2.6 Cell culture

The NG108-15 (neuroblastoma X glioma) hybrid cells were grown in high-glucose Dulbecco's modified Eagle's medium supplemented with 10% foetal bovine serum, penicillin G, and streptomycin. The cultures were maintained at 37°C in a humidified atmosphere of 5% CO_2. Cells were seeded in six-well plates and grown until 60–70% confluent before treatment with increasing concentrations of Ang II (6.25–100 μM), Los (1 μM), or both for 24 h.

2.7 Real-time PCR, western blotting, and immunofluorescent staining for nNOS and CAPON

Samples of PVN were obtained using the micropunch technique of Palkovits[2,11,17,21,25] to determine mRNA and protein expression of nNOS and CAPON. These samples were subsequently subjected to routine real-time PCR and western blot analysis of CAPON and nNOS in the PVN. Sections of the PVN were also subjected to immunofluorescent staining to visualize the distribution of nNOS and CAPON within the PVN. Similar experimental techniques were utilized to examine CAPON and nNOS in NG108 cells *in vitro*. The details of the real-time PCR, western blotting, and immunostaining techniques are provided in Supplementary material online.

2.7.1 Co-immunoprecipitation

CAPON was immunoprecipitated from NG108 cell lysates using CAPON antisera and subsequently analysed by western blot to examine the co-immunoprecipitation of nNOS and CAPON. Greater details of the method are described in the Supplementary material online.

2.7.2 siRNA knockdown

siRNA targeting CAPON, a negative control siRNA, was purchased from Invitrogen. Transient transfection was performed in NG108 cells using Lipofectamine 2000 as per the manufacturer's instructions.

2.8 Data analyses

The data were expressed as mean ± SEM and statistical significance was set at $P \leq 0.05$. Statistical comparisons of two groups were made using a Student's *t*-test. Differences between multiple groups were determined by two-way ANOVA followed by a Student–Newman–Keuls test for *post hoc* analysis of significance.

3. Results

3.1 Characteristics of sham and CHF groups

Table 1 summarizes the salient morphological and haemodynamic characteristics of sham and CHF groups. The infarcted area in the CHF group was ~37% of the endocardial surface. Sham rats had no observable damage of the myocardium. LVESD and LVEDD

Table 1 Characteristics of four groups of rats in the microinjection and molecular biological experiments

	Sham + Veh ($n = 6$)	CHF + Veh ($n = 7$)	Sham + Los ($n = 6$)	CHF + Los ($n = 6$)
Body weight (g)	389 ± 21	405 ± 16	378 ± 8	389 ± 11
Infarct size (% of left ventricle)	0	37 ± 5*	0	37 ± 3*
LVESD (mm)	2.6 ± 0.3	6.4 ± 0.3*	3.1 ± 0.5	6.3 ± 0.3*
LVEDD (mm)	6.0 ± 0.3	10.2 ± 0.7*	6.7 ± 0.5	9.9 ± 0.7*
EF (%)	79 ± 3	48 ± 3*	81 ± 7	51 ± 12*
LVEDP (mmHg)	4.5 ± 1.3	23.1 ± 3.8*	6.3 ± 1.2	15.4 ± 2.9*,#
dP/dt (mmHg/s)	8456 ± 256	5187 ± 367*	8508 ± 416	5690 ± 428*
Basal RSNA (% of max)	21.2 ± 2.7	37.4 ± 8.5*	18.9 ± 3.6	28.8 ± 2.25*,#

*$P < 0.05$ vs. sham group.
#$P < 0.05$ vs. vehicle-treated CHF group.

were significantly increased in the CHF + vehicle (Veh) group compared with the sham + Veh group. Los treatment in the CHF + Los group had no effect on LVESD but attenuated LVEDD compared with CHF + Veh, although LVEDD was still significantly elevated compared with both sham groups. EF was decreased in the CHF + Veh and CHF + Los groups compared with the sham + Veh and sham + Los groups. LVEDP was significantly elevated in the CHF + Veh group compared with the sham + Veh group. LVEDP in the CHF + Los group was significantly attenuated compared with the CHF + Veh group but was still significantly higher than that in the sham + Veh and sham + Los groups. d*P*/d*t* was significantly decreased in both the CHF + Veh and CHF + Los groups compared with both the sham + Veh and sham + Los groups, indicating a decreased contractility that resulted in an increase in LVEDP. Taken together, the ≥30% infarct size increased LVEDP, LVESD, and LVEDD and decreased d*P*/d*t* and EF, indicating that rats in both CHF groups were experiencing cardiac dysfunction.

3.2 Expression of CAPON and nNOS in the PVN

CAPON expression at the transcriptional level was determined by real-time PCR in the PVN of the four groups (*Figure 1*). Relative CAPON mRNA was appreciably higher in the punched PVN tissues from CHF group compared with the sham group. CAPON mRNA expression in the CHF + Los group was significantly attenuated when compared with the CHF group and was nearly the same as in the sham or sham + Los groups (*Figure 1A*). These data indicate that chronic AT_1 receptor blockade by Los normalizes/prevents/annuls the increased CAPON mRNA expression in the PVN of rats with CHF. *Figure 1B* and *C* shows CAPON and nNOS protein expression in the PVN in the four groups. Consistent with the increased mRNA level, CAPON protein expression in the PVN of CHF rats was considerably higher than that in the sham group. CAPON protein expression in the CHF + Los group was reduced compared with the CHF group and was not significantly different from the sham + Los group. On the other hand, nNOS protein expression was significantly reduced in the PVN of the CHF group compared with the sham group, consistent with our previous data showing a decreased nNOS expression level in the PVN.[11,26] However, nNOS protein expression in the CHF + Los group was restored when compared with the CHF group and was not significantly different from the sham and sham + Los groups. These data indicate that chronic AT_1 receptor blockade by Los blocks up-regulation of CAPON and concomitant down-regulation of nNOS.

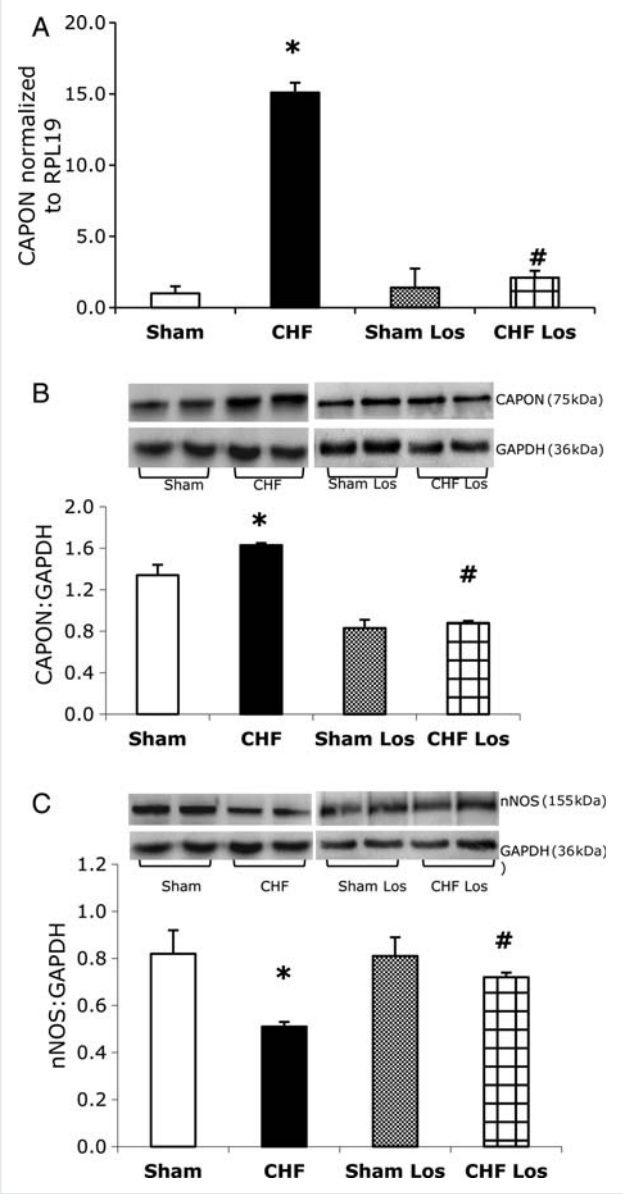

Figure 1 mRNA expression of CAPON (*A*) relative to rpl19 in the PVN measured by real-time PCR in sham and CHF groups. Western blot analysis of CAPON (*B*) and nNOS (*C*) protein in the PVN of sham and CHF groups. Top: a representative gel, bottom: densitometry analyses of CAPON protein level normalized to GAPDH. Values are mean ± SE of quadruplicate analyses of four to five rats in each group. Changes in CAPON mRNA are presented in folds with reference to the sham group. $^{*}P < 0.05$ vs. sham. $^{\#}P < 0.05$ vs. CHF.

3.3 Immunohistochemical examination of CAPON and nNOS in the PVN

To corroborate the biochemical data that there is an increase in CAPON expression with a concomitant decrease in nNOS in the PVN, sections of the PVN were stained for nNOS and CAPON, *in situ*, in sham and CHF rats (*Figure 2*). As assessed visually, nNOS immunostaining was less intense while CAPON was brighter in ventromedial parvocellular subnucleus as well as in the magnocellular portions of the PVN in CHF rats when compared with sham rats.

3.4 Microinjection of NOS inhibitor L-NMMA into the PVN

Basal RSNA, calculated as per cent of maximum, was significantly increased in rats with CHF and was significantly reduced in CHF rats treated with Los (*Table 1*). The administration of L-NMMA into the PVN elicited a dose-dependent increase in RSNA, MAP, and HR in sham and CHF rats (*Figure 3*). At all three doses of L-NMMA, the increase in RSNA was significantly less in the CHF + Veh group compared with other groups (*Figure 3B*). At 50 pmol, the response

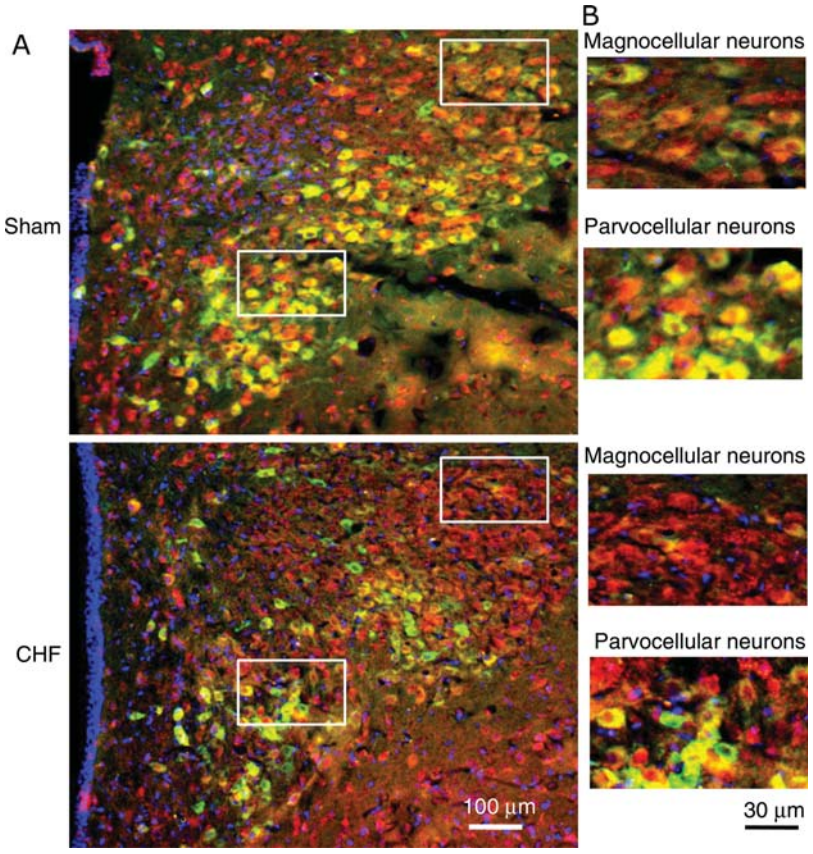

Figure 2 Immunofluorescent photomicrographs from the sections of the PVN region, (*A*) lower magnification; (*B*) higher magnification, lateral magnocellular subnucleus; ventromedial parvocellular subnucleus stained for CAPON (red) and nNOS (green) in sham and CHF rats. Nuclei (blue) are stained by DAPI.

in the CHF + Veh group was 7.6 ± 1.1 ($n = 7$), which was significantly lower than that in the sham + Veh (15.0 ± 1.6, $n = 6$), sham + Los (11.5 ± 1.2, $n = 6$), and CHF + Los (11.9 ± 0.4, $n = 6$) groups. Although basal RSNA was increased in CHF rats, the delta increases in RSNA to L-NMMA were still significantly less in rats with CHF. Los treatment significantly increased the blunted response to L-NMMA microinjected into the PVN in rats with CHF. *Figure 3C* and *D* shows the increase in MAP and HR in response to increasing doses of L-NMMA microinjected into the PVN. The increase in MAP and HR in the CHF group was significantly lower compared with the sham and CHF + Los groups. There were no significant differences in any of the parameters monitored between the sham + Los and CHF + Los groups.

3.5 Effect of Ang II on nNOS and CAPON protein expression in NG108 cells

NG108 cells were treated with different concentrations of Ang II and changes in nNOS and CAPON protein expression were analysed by western blot analysis after 24 h (*Figure 4*). nNOS protein expression was down-regulated significantly even at the lower concentrations of Ang II (*Figure 4A*). Treatment with Los for 1 h prior to Ang II treatment for 24 h prevented the decrease in nNOS expression (*Figure 4B*). In contrast to nNOS, CAPON expression (CAPON/GAPDH) increased with an increasing concentration of Ang II compared with control (*Figure 4C*). CAPON expression increased in a dose-dependent manner and the increase was statistically significant at 50 μM (33%) and 100 μM Ang II (40%). Treatment with Los significantly ameliorated increased CAPON expression (*Figure 4D*).

3.6 Subcellular co-localization and interactions of CAPON and nNOS in NG108 cells

CAPON and nNOS subcellular localization and their interaction in NG108 cells were examined by immunofluorescence microscopy (*Figure 5A*) and co-immunoprecipitation experiments (*Figure 5B*). The intensity of CAPON (red) was increased while of nNOS (green) was decreased with 100 μM Ang II treatment, indicating that Ang II down-regulated the expression of nNOS and up-regulated the expression of CAPON in NG108 cells. To further examine the association between CAPON and nNOS, we performed co-immunoprecipitation experiments in NG108 cell lysates (*Figure 5B*). Immunoprecipitation with an anti-CAPON antibody and immunoblotting with an anti-nNOS antibody demonstrated that CAPON and nNOS physically interacted with each other in Ang II-treated as well as control NG108 lysates, suggesting a direct or an indirect interaction of CAPON and nNOS. Moreover, siRNA-mediated gene silencing of CAPON in NG108 cells showed an approximately three-fold increase in the nNOS expression level,

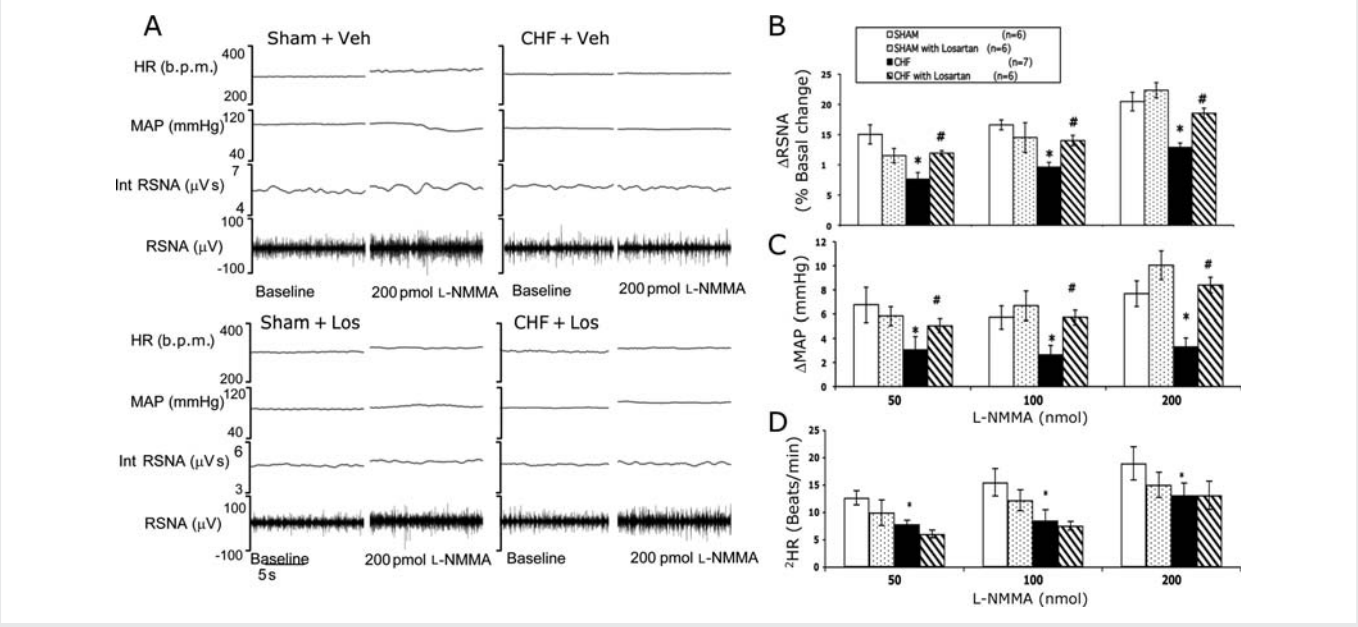

Figure 3 RSNA, MAP, and HR responses to L-NMMA injected into the PVN. (*A*) Segment of an original recording from an individual rat demonstrating the baseline parameters and peak changes in RSNA, integrated RSNA, MAP, and HR by administration of 200 pmol L-NMMA into the PVN in the four groups: sham + Veh, CHF + Veh, sham + Los, and CHF + Los. Mean data of changes in (*B*) RSNA, (*C*) MAP, and (*D*) HR following increasing doses of L-NMMA into the PVN of the four groups. $^{*}P < 0.05$ vs. sham. $^{\#}P < 0.05$ vs. CHF.

suggesting a functional significance of CAPON and nNOS interaction (*Figure 5C*).

4. Discussion

The novel finding of this study is that there is an enhanced expression of CAPON with a concomitant decrease in nNOS in the PVN of rats with CHF, which are reversed by AT_1 receptor blocker Los. The endogenous levels of nNOS are also restored to normal after AT_1 receptor blockade, showing normal responses in changes in RSNA to blockade of NOS in the PVN. Further, using the NG108 neuronal cells, our findings demonstrate that Ang II via AT_1 receptors up-regulates CAPON with a concomitant decrease in the expression of nNOS. Taken together, these data demonstrate that elevated levels of Ang II in CHF cause up-regulation of CAPON in the PVN, which sequesters nNOS resulting in reduced inhibitory influence and thus causes an overactivation of the sympatho-excitatory drive from the PVN in CHF.

This study used a coronary artery ligation model of CHF, which mimics a reliable and consistent simulation of the CHF condition.[17,22,26] CHF was demonstrated by increased LVEDP, decreased dP/dt of the left ventricle, decreased EF, and >30% infarct of the left ventricle at the time of experiment. The advantage of using this model as opposed to other models of CHF, such as ventricular pacing, is that it mimics/simulates the blockade of the coronary artery, commonly observed in patients with CHF.

In our previous studies, we had shown a decreased nNOS mRNA and protein expression in the PVN of rats with heart failure.[11,26] The lower level of nNOS in the PVN leads to a decrease in NO production, which contributes to an increase in sympathetic outflow.[27,28] Subcellular fractionation of the brain showed that approximately half of nNOS was soluble while the other half was associated with membrane fraction.[29] Membrane proteins, such as synotrophin, PSD95, or PSD93, are highly expressed in synaptic densities and interact with nNOS through PDZ domains.[29,30] The nNOS/PSD95 interaction involves the unique PDZ domain of nNOS and the second PDZ domain of PSD95.[30] The linkage of NMDA receptors to nNOS by PSD95 increases the availability of calcium to nNOS leading to tightly coupled nNOS activation, following NMDA receptor activation and subsequent inflow of calcium.[13] CAPON competes with PSD95 for interaction with nNOS through its carboxy terminus, and overexpression of CAPON results in loss of PSD95/nNOS complexes[13] which causes uncoupling of the NMDA–nNOS–NO-mediated signalling pathway. CAPON has also been shown to selectively interact with monomeric G-proteins Dexras1[31] and synapsin[16] via the PTB domain. This suggests a role of CAPON in regulating downstream signal transduction pathways; CAPON has also been implicated in neurotransmitter release and neuronal plasticity under normal and pathological conditions.[32] In the present study, we observed increased levels of CAPON with concomitant decrease in nNOS in the PVN of rats with CHF. These findings suggest that the decrease in nNOS is due to increased CAPON expression, which in turn sequesters nNOS. The inactivation of nNOS by CAPON then leads to less NO-mediated inhibitory action on sympathetic outflow in CHF.

We recently reported an increase in the expression of NMDA-NR_1 receptors in the PVN of rats with CHF.[21] The functional NMDA receptor comprises NR_1 and NR_2 subunits. The NR_2B subtype has been reported to be expressed at a higher level compared with NR_2A, NR_2C, and NR_2D in the parvocellular subdivisions of the PVN.[33] The expression of these other NR_2 subtypes may also increase in CHF, but this remains to be determined. Nevertheless,

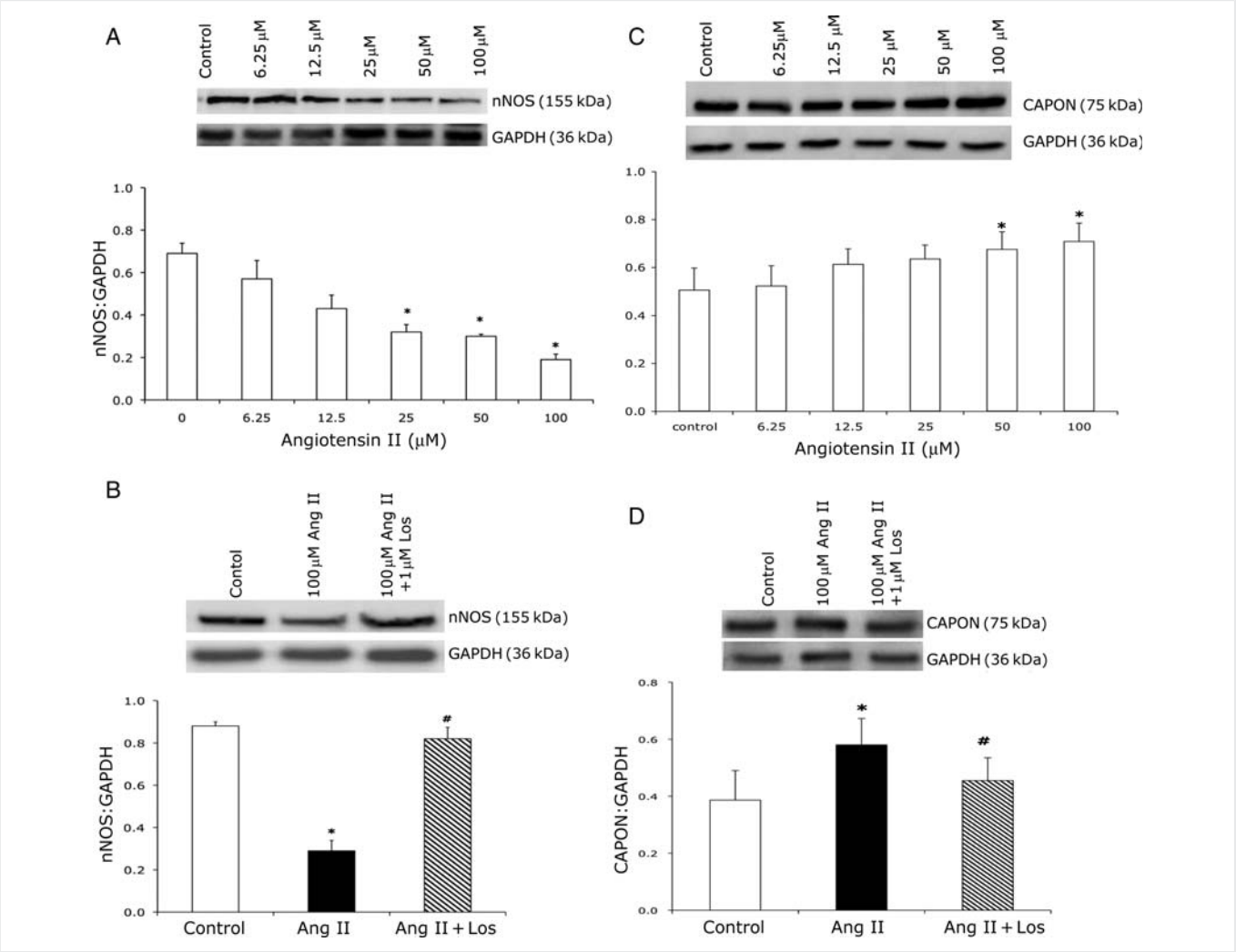

Figure 4 (*A*) Expression of nNOS with increasing doses of Ang II in NG108 cell line. Top: a representative gel, bottom: densitometry analyses of nNOS protein level normalized to GAPDH. (*B*) Expression of nNOS in control, Ang II-treated, and Ang II + Los-treated NG108 cells. Top: a representative gel, bottom: densitometry analyses of nNOS protein level normalized to GAPDH. (*C*) Expression of CAPON with increasing doses of Ang II in NG108 cells. Top: a representative gel, bottom: densitometry analyses of CAPON protein level normalized to GAPDH. (*D*) Expression of CAPON in control, Ang II-treated and Ang II + Los-treated NG108 cells. Top: a representative gel, bottom: densitometry analyses of CAPON protein level normalized to GAPDH. Values were mean ± SE from four independent experiments. $^{*}P < 0.05$ vs. control. $^{\#}P < 0.05$ vs. Ang II-treated cells.

NMDA stimulation of the PVN produces a bigger sympathoexcitation in rats with CHF compared with sham rats, suggesting that the NMDA receptor-mediated changes in RSNA are elevated in the CHF condition. Moreover, the blockade of NMDA receptor in the PVN induced greater decreases in RSNA, arterial pressure, and HR in rats with CHF compared with sham rats, which suggests that endogenous glutamatergic tone is significantly increased in CHF.[11] The blockade of AT_1 receptors has been shown to prevent this increased glutamatergic tone in CHF. It is possible that CAPON indirectly alters the NMDA receptor activity through activation of the AT_1 receptor.

The role of CAPON has been extensively studied in schizophrenia with regard to glutamate neurotransmission known to be involved in this disease.[34] The long form of CAPON (CAPON-L), functionally reacts with nNOS in neurons to affect activity and stability[13,35] and was found to be increased in patients with schizophrenia and bipolar disorders.[36] Interestingly, NOS-expressing PVN neurons are significantly reduced in schizophrenic and depressive patients when compared with control patients,[37] similar to what we have observed here in rats with CHF. Interestingly, the CAPON-L appears to be linked with nNOS in the current studies. nNOS expression has also been shown to be altered in other human brain areas of patients with schizophrenia and depression.[38]

There is a high correlation between co-morbidity of depression and heart disease.[39] However, the cause(s) for this high correlation is not known. Depression is an established risk factor for heart disease[40] and 50% of the patients with CHF are depressed.[39] It is tempting to speculate that the central pathways involved in CHF and depression/schizophrenia may utilize nNOS and CAPON as part of neural circuitry for central processing. Alterations in CAPON and nNOS described here in the PVN may be common features of this abnormality in these pathways and other central pathways. Thus, we postulate that there

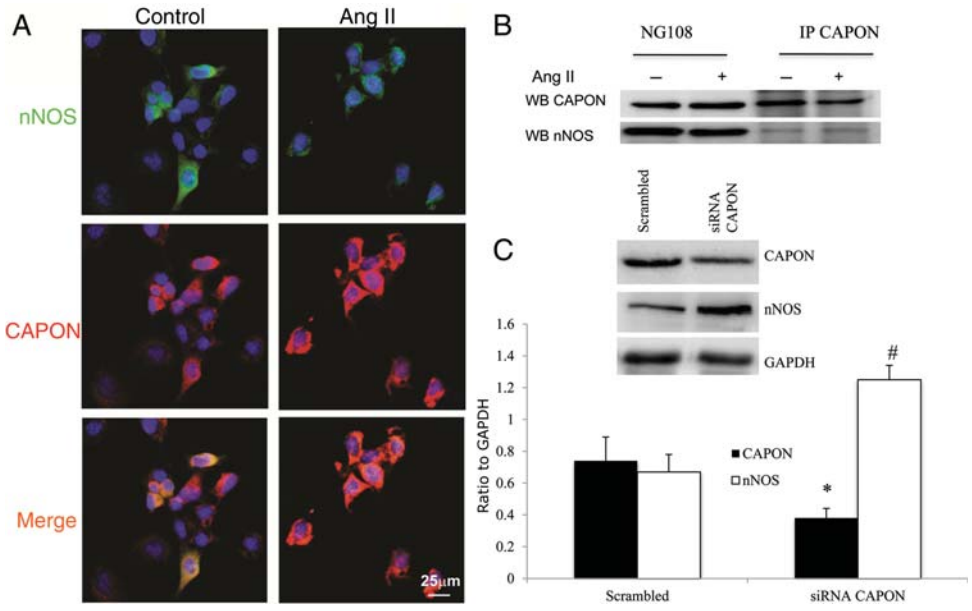

Figure 5 (*A*) Immunocytochemical localization of CAPON and nNOS in NG108 cells in control and 100 μM Ang II-treated NG108 cells. nNOS (green), CAPON (red), and nuclei (blue). (*B*) Immunoprecipitation of CAPON in control and Ang II-treated NG108 cell lysate. (*C*) Knockdown of CAPON in NG108 cell line with siRNA CAPON. Top: a representative gel, bottom: densitometry analyses of CAPON and nNOS protein level normalized to GAPDH. Values were mean ± SE from four independent experiments. $^{*}P < 0.05$ vs. scrambled CAPON. $^{\#}P < 0.05$ vs. scrambled nNOS.

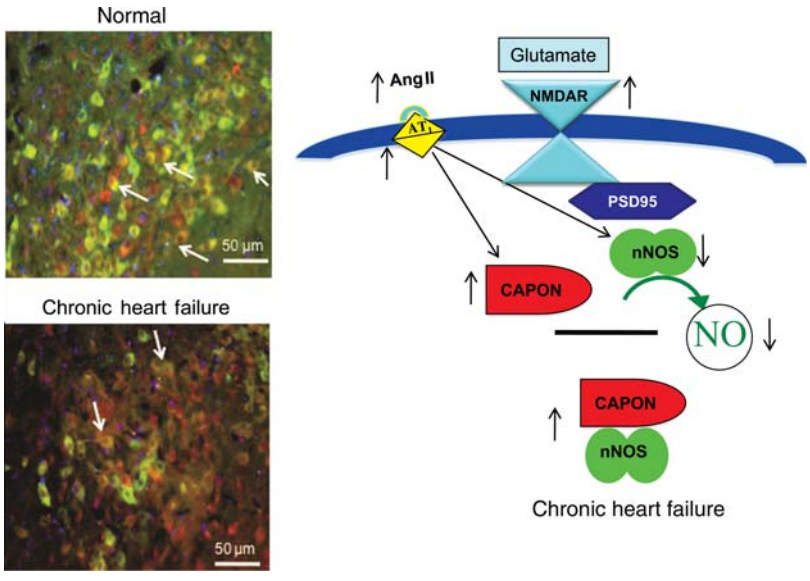

Figure 6 A proposed model for the down-regulation of nNOS by CAPON in the PVN by Ang II during CHF. Normal activation of NMDA receptor leads to Ca^{2+} entry. Due to the PSD95/nNOS complex, nNOS is placed in proximity to the entering Ca^{2+} leading to Ca^{2+}–calmodulin-induced activation of nNOS and thus the production of NO. In the CHF condition, there is an overexpression of CAPON due to increased Ang II levels as well as increased AT_1 receptors in the PVN. CAPON competes with PSD95 for binding to nNOS. The increased CAPON in CHF leads to increased binding of CAPON to nNOS resulting in CAPON sequestering nNOS and decreasing NMDAR/PSD95/nNOS complexes, which attenuates Ca^{2+}-dependent activation of nNOS, leading to a catalytically inactive nNOS in CHF. This then results in reduced production of NO in the CHF. Micrograph depicts the decreased expression of nNOS and increased expression of CAPON in the PVN sections from CHF compared with sham rats.

may be points of convergence within the CNS, such as CAPON and nNOS within neurons that are common abnormalities for these disorders. The identification of candidate mediators, such as CAPON and nNOS, common to heart disease and depression/schizophrenia may serve as an important convergence point for research in investigating why these disorders are so frequently co-morbid. Our findings may form the basis for examination of this convergence in these diseases.

Our findings also showed that in rats with CHF, 3-week Los treatment normalized the increased CAPON levels in the PVN. Subsequent *in vitro* studies showed that Los treatment prevented Ang II-mediated increases in CAPON levels within 24 h. These data suggest that the effects of Ang II blockade with Los are likely due to a short-term effect rather than a long-term plasticity phenomenon on PVN neurons; however, this possibility remains to be examined further. Ang II is known to enhance the reactive oxygen species (ROS) in the brain.[41] Moreover, elevated cytokines in the PVN also induce production of ROS in the neurons increasing the sympatho-excitatory effect.[42] We have already documented that Los treatment in rats with CHF normalized the increased mRNA and protein expression of the NMDA receptor subunit NR_1.[21] Taken together, this led us to hypothesize that there may be some cross-talk among cytokine, ROS, AT_1 receptor, and NMDA receptor in CHF that leads to increased expression of CAPON mRNA and protein to functionally regulate nNOS expression. CAPON competes with PSD95 for binding with nNOS and overexpression of CAPON sequesters the available nNOS (*Figure 6*). CAPON may reduce cellular NO production by regulating nNOS activity or switch it towards the degradation pathway by post-translational modifications such as ubiquitination so that neuroprotective rather than neurotoxic NO levels are produced under diseased condition such as CHF.

In the present study, Ang II treatment of NG108 neuronal cells results in down-regulation of nNOS and up-regulation of CAPON expression, indicating that Ang II might regulate the CAPON-induced signalling cascade. Ang II is known to activate p38 mitogen-activated protein kinase, extracellular signal-regulated protein kinase, and stress-activated protein kinase/Jun N-terminal kinase, which are involved in the regulation of gene expression.[43] The possible role of transcription factors viz. activator protein 1 (c-jun, c-Fos), NFκB, SP1, CREB, and Raf-1, downstream of the above-mentioned signalling pathways on nNOS and CAPON transcription in CHF rats, remains to be examined.

In summary, our studies have revealed that nNOS and CAPON co-localize in the pre-sympathetic autonomic neurons in the PVN and their expression is reciprocally regulated in CHF. We hypothesized that overexpression of CAPON, caused by increased Ang II via AT_1 receptors, in the PVN sequesters nNOS, results in decreases in nNOS leading to decreased production of NO and increases sympathoexcitation (*Figure 6*). This lack of the inhibitory feedback by NO production allows for exaggerated glutamatergic tone in the PVN of rats with CHF. Further, investigation into the Ang II driven, CAPON-mediated molecular mechanism/s for down-regulation of nNOS will provide new insights with regard to the regulation of nNOS in CHF. Perhaps, the insights gained about these mechanisms can be used as possible therapeutic targets for complications of the CHF condition specifically and, more broadly, for patients with an affective disorder (depression) and schizophrenia in other parts of the brain.

Supplementary material

Supplementary material is available at *Cardiovascular Research* online.

Acknowledgements

The technical assistance of Kurtis Cornish and Xuefei Liu is greatly appreciated.

Conflict of interest: none declared.

Funding

Funding from National Institutes of Health, Heart, Lung, and Blood Institute, grant HL62222, supported the work.

References

1. Packer M. Neurohormonal interactions and adaptations in congestive heart failure. *Circulation* 1988;**77**:721–730.
2. Li YF, Cornish KG, Patel KP. Alteration of NMDA NR1 receptors within the paraventricular nucleus of hypothalamus in rats with heart failure. *Circ Res* 2003;**93**:990–997.
3. Zheng H, Li Y-F, Wang W, Patel KP. Enhanced angiotensin-mediated excitation of renal sympathetic nerve activity within the paraventricular nucleus of anesthetized rats with heart failure. *Am J Physiol Regul Integr Comp Physiol* 2009;**297**:R1364–R1374.
4. Hasking GJ, Esler MD, Jennings GL, Burton D, Korner PI. Norepinephrine spillover to plasma in patients with congestive heart failure: evidence of increased overall and cardio-renal sympathetic nervous activity. *Circulation* 1986;**73**:615–621.
5. Liu JL, Irvine S, Reid IA, Patel KP, Zucker IH. Chronic exercise reduces sympathetic nerve activity in rabbits with pacing-induced heart failure—a role for angiotensin II. *Circulation* 2000;**102**:1854–1862.
6. Patel KP, Zhang PL, Krukoff TL. Alterations in brain hexokinase activity associated with heart failure in rats. *Am J Physiol Regul Integr Comp Physiol* 1993;**265**:R923–R928.
7. Kannan H, Niijima A, Yamashita H. Effects of stimulation of the hypothalamic paraventricular nucleus on blood pressure and renal sympathetic nerve activity. *Brain Res Bull* 1988;**20**:779–783.
8. Swanson LW, Sawchenko PE. Paraventricular nucleus: a site for the integration of neuroendocrine and autonomic mechanisms. *Neuroendocrinology* 1980;**31**:410–417.
9. Commons KG, Pfaff DW. Ultrastructural evidence for enkephalin mediated disinhibition in the ventromedial nucleus of the hypothalamus. *J Chem Neuroanat* 2001;**21**:53–62.
10. Zhang K, Mayhan WG, Patel KP. Nitric oxide within the paraventricular nucleus mediates changes in renal sympathetic nerve activity. *Am J Physiol* 1997;**273**:R864–R872.
11. Li Y-F, Patel KP. Paraventricular nucleus of the hypothalamus and elevated sympathetic activity in heart failure: altered inhibitory mechanisms. *Acta Physiol Scand* 2003;**177**:17–26.
12. Schuman EM, Madison DV. Nitric oxide and synaptic function. *Ann Rev Neurosci* 1994;**17**:153–183.
13. Jaffrey SR, Snowman AM, Eliasson MJ, Cohen NA, Snyder SH. CAPON: a protein associated with neuronal nitric oxide synthase that regulates its interactions with PSD95. *Neuron* 1998;**20**:115–124.
14. Bredt DS, Synder SH. Nitric oxide mediates glutamate-linked enhancement of cGMP levels in the cerebellum. *Proc Natl Acad Sci USA* 1989;**86**:9030–9033.
15. Garthwaite J, Garthwaite G, Palmer RMJ, Moncada S. NMDA receptor activation induces nitric oxide synthesis from arginine in rat brain slices. *Eur J Pharmacol* 1989;**172**:413–416.
16. Jaffrey SR, Benfenati F, Snowman AM, Czernik AJ, Snyder SH. Neuronal nitric-oxide synthase localization mediated by a ternary complex with synapsin and CAPON. *Proc Natl Acad Sci USA* 2002;**99**:3199–3204.
17. Kleiber AC, Zheng H, Schultz HD, Peuler JD, Patel KP. Exercise training normalizes enhanced glutamate-mediated sympathetic activation from the PVN in heart failure. *Am J Physiol Regul Integr Comp Physiol* 2008;**294**:R1863–R1872.
18. Li YF, Wang W, Mayhan WG, Patel KP. Angiotensin-mediated increase in renal sympathetic nerve discharge within the PVN: role of nitric oxide. *Am J Physiol Regul Integr Comp Physiol* 2006;**290**:R1035–R1043.
19. Kinugawa T, Ogino K, kitamura H, Saitoh M, Omodani H, Osaki S *et al*. Catecholamines, renin–angiotensin–aldosterone system, and atrial natriuretic peptide at rest and during submaximal exercise in patients with congestive heart failure. *Am J Med Sci* 1996;**312**:110–117.
20. Sumners C, Fleegal MA, Zhu M. Angiotensin AT_1 receptor signalling pathways in neurons. *Clin Exp Pharmacol Physiol* 2002;**29**:483–490.
21. Kleiber AC, Zheng H, Sharma NM, Patel KP. Chronic AT_1 receptor blockade normalizes NMDA-mediated changes in renal sympathetic nerve activity and NR_1 expression within the PVN in rats with heart failure. *Am J Physiol Heart Circ Physiol* 2010;**1152**:1546–1555.
22. Zhang K, Patel KP. Effect of nitric oxide within the paraventricular nucleus on renal sympathetic nerve discharge: role of GABA. *Am J Physiol* 1998;**275**:R728–R734.

23. Goncalves ARR, Fujihara CK, Matter AL, Malheiros DMAC, Noronha IL, De Nucci G *et al*. Renal expression of COX-2, Ang II, and AT1 receptor in remnant kidney: strong renoprotection by therapy with losartan and a nonsteroidal anti-inflammatory. *Am J Physiol* 2004;F945–F954.
24. Paxinos G, Watson C. *The Rat Brain in Stereotaxic Coordinates*. 2nd ed. Orlando: Academic Press, 1986.
25. Palkovits M, Brownstein M. Brain microdissection techniques. In: Cuello AE, ed. *Brain Microdissection Techniques*. Chichester: John Wiley & Sons, 1983.
26. Zheng H, Li YF, Cornish KG, Zucker IH, Patel KP. Exercise training improves endogenous nitric oxide mechanisms within the paraventricular nucleus in rats with heart failure. *Am J Physiol Heart Circ Physiol* 2005;**288**:H2332–H2341.
27. Patel KP, Li YF, Hirooka Y. Role of nitric oxide in central sympathetic outflow. *Proc Soc Exp Biol Med* 2001;**226**:814–824.
28. Li YF, Roy SK, Channon KM, Zucker IH, Patel KP. Effect of *in vivo* gene transfer of nNOS in the PVN on renal nerve discharge in rats. *Am J Physiol Heart Circ Physiol* 2002;**282**:H594–H601.
29. Bredt DS. Targeting nitric oxide to its targets. *Proc Soc Exp Biol Med* 1996;**211**:41–48.
30. Brenman JE, Chao DS, Gee SH, McGee AW, Craven SE, Santillano DR *et al*. Interaction of nitric oxide synthase with the postsynaptic density protein PSD-95 and alpha-1 syntrophin mediated by PDZ domains. *Cell* 1996;**84**:757–767.
31. Fang MJS, Sawa A, Ye K, Luo X, Snyder SH. Dexras1: a G protein specifically coupled to neuronal nitric oxide synthase via CAPON. *Neuron* 2000;**28**:183–193.
32. Che YH, Tamatani M, Tohyama M. Changes in mRNA for post-synaptic density-95 (PSD-95) and carboxy-terminal PDZ ligand of neuronal nitric oxide synthase following facial nerve transection. *Mol Brain Res* 2000;**76**:325–335.
33. Herman JP, Eyigor O, Ziegler DR, Jennes L. Expression of ionotropic glutamate receptor subunit mRNAs in the hypothalamic paraventricular nucleus of the rat. *J Comp Neurol* 2000;**422**:352–362.
34. Coyle JT, Tsai G, Goff D. Converging evidence of NMDA receptor hypofunction in the pathophysiology of schizophrenia. *Ann N Y Acad Sci* 2003;**1003**:318–327.
35. Chang KC, Barth AS, Sasano T, Kizana E, Kashiwakura Y, Zhang Y *et al*. CAPON modulates cardiac repolarization via neuronal nitric oxide synthase signaling in the heart. *Proc Natl Acad Sci USA* 2008;**105**:4477–4482.
36. Carrel D, Du Y, Komlos D, Hadzimichalis NM, Kwon M, Wang B *et al*. NOS1AP regulates dendrite patterning of hippocampal neurons through a carboxypeptidase E-mediated pathway. *J Neurosci* 2009;**29**:8248–8258.
37. Bernstein HG, Stanarius A, Baumann B, Henning H, Krell D, Danos P *et al*. Nitric oxide synthase-containing neurons in the human hypothalamus: reduced number of immunoreactive cells in the paraventricular nucleus of depressive patients and schizophrenics. *Neuroscience* 1998;**83**:867–875.
38. Karson CN, Griffin WS, Mrak RE, Husain M, Dawson TM, Snyder SH *et al*. Nitric oxide synthase (NOS) in schizophrenia: increases in cerebellar vermis. *Mol Chem Neuropathol* 1996;**27**:275–284.
39. Johnson AK, Grippo AJ. Sadness and broken hearts: neurohumoral mechanisms and co-morbidity of ischemic heart disease and psychological depression. *J Physiol Pharmacol* 2006;**57**:5–29.
40. *Depression Can Break Your Heart*. NIH Publication No. 01-4592. Bethesda: National Institute of Mental Health.
41. Zimmerman MC, Lazartigues E, Lang JA, Sinnayah P, Ahmad IM, Spitz DR *et al*. Superoxide mediates the actions of angiotensin II in the central nervous system. *Circ Res* 2002;**91**:1038–1045.
42. Guggilam A, haque M, Kerut EK, McIlwain E, Lucchesi P, Seghal I *et al*. TNF-alpha blockade decreases oxidative stress in the paraventricular nucleus and attenuates sympathoexcitation in heart failure rats. *Am J Physiol Heart Circ Physiol* 2007;**293**:H599–H609.
43. Omura T, Yoshiyama M, Matsumoto R, Kusuyama T, Enomoto S, Nishiya D *et al*. Role of c-Jun NH2-terminal kinase in G-protein-coupled receptor agonist-induced cardiac plasminogen activator inhibitor-1 expression. *J Mol Cell Cardiol* 2005;**38**:583–592.